



SEISMIC PERFORMANCE ASSESSMENT OF A SEGMENTAL TRI-CELLULAR BOX GIRDER BRIDGE

A. Viviescas⁽¹⁾, A. Zapata-García⁽²⁾, C.A. Riveros-Jerez⁽³⁾

⁽¹⁾ Professor, Industrial University of Santander. Bucaramanga, (Colombia), alvivija@uis.edu.co

⁽²⁾ Civil Engineer, University of Antioquia. Medellín, (Colombia), arlen.zapata@udea.edu.co

⁽³⁾ Associate Professor, University of Antioquia. Medellín, (Colombia), carlos.riveros@udea.edu.co

Abstract

Colombia is experiencing a rapid economic growth leading to construction of several bridges to interconnect major economic regions mainly located in high or intermediate seismic zones. The percentage of national population living in seismic areas is approximately 87% highlighting the importance of appropriate implementation of seismic design considerations in order to guarantee adequate infrastructure investment. Although the Colombian Bridge Construction Code [1] allows multiple level design using multiple return periods depending on owners, bridges in Colombia are mainly designed using a single level design defined by the 1000-year return period adopted from the LRFD Specifications [2] and the LRFD Guide Specifications for Seismic Bridge Design [3]. The number of bridges constructed in Colombia have increased in recent years and the main feature related to current Colombian bridge construction is that the most widely used structural configuration corresponds to segmental box girder bridge, whose design is mainly based on elastic models and therefore relies on the correct determination of the seismic response modification factor. The Yatí-Bodega bridge was constructed to connect the Magangué with Mompox cities becoming in 2020 the largest bridge in South America with a total length of 2.3 Km, the bridge located over the Magdalena's river was constructed using segmental bridge construction. The 1995 Kobe and 2011 Tohoku earthquakes resulted in huge economic losses and highlighted the necessity to address serviceability of bridges after major earthquake events leading to new versions of bridge codes such as the Japanese Code [4] and the Canadian Highway Bridge Design Code [5] by incorporating the use of quantitative criteria to evaluate the seismic bridge performance. The segmental bridge selected in this study corresponds to the main bridge structure of the La Union viaduct located in Bucaramanga, Colombia and having a central length of 111 m. and lateral lengths of 52.45 m and 55.5 m. The superstructure of the central bridge is supported by two pairs of columns. The geometry selected for the columns corresponds to a rectangular hollow prismatic with an external cross section of 6 m x 5 m, and an internal cross section of 5 m x 4 m, provided with a constant wall thickness of 0.5 m. The pair of columns are separated to each other at a center-to-center distance of 11.2 m, with a height of 22 m. The cross section of the bridge corresponds to a tricellular concrete box girder of varying height (2.5 m to 6 m) and constant width of 22.5 m. This seismic performance assessment of La Union viaduct is carried out using prescriptions provided by the [5] and the British Columbia (Canada) Ministry of Transportation and Infrastructure [6]. The numerical results obtained from a fiber-based finite element model using adaptive pushover and time history nonlinear analysis are compared in terms of the design criteria and damage limit states provided by the bridge codes [5] and [6]. The adaptive pushover analysis results show ductility reserve after reaching the serviceability limit in the longitudinal direction. However, the ductility level is very limited in the transverse direction reaching the ultimate limit state soon after the serviceability limit is achieved. This result is in accordance with the value of the seismic modification factor ($R=1.0$) used in the design. The nonlinear time history time results show adequate seismic performance of the bridge columns. It was possible to verify the seismic performance of the bridge at the serviceability level using the design level defined by the 1000-year return period. No damage is induced in the columns due to the effect of the scaling ground motions acting on the bridge.

Keywords: Segmental bridge; tri-cellular box girde; static-nonlinear analysis; nonlinear time history analysis; seismic response modification factor.



1. Introduction

Colombia economic growth depends in part on improving the connectivity to international markets through the construction of modern transportation networks. Road infrastructure plays a major role in connecting major national centers of commerce and industry due to the national mountainous topography and lack of rail infrastructure development. On the other hand, construction of river port infrastructure is still too slow to meet national economic demands. The percentage of national population living in seismic areas is approximately 87% highlighting the importance of appropriate implementation of seismic design considerations in order to guarantee adequate infrastructure investment. In addition, modern road design standards are undergoing a continuous evolution demanding long-lasting infrastructure and environmentally friendly construction practices. Bridge engineering has been strongly linked to relevant advances in areas such as materials, construction processes, and modeling. Thus, segmental bridge construction has been widely used and therefore becoming a safe and economical construction process that can be implemented in a variety of difficult site conditions providing very economical solutions for long spans (over 100 meters), especially when access to the construction site is limited. The use of nonlinear procedures in seismic assessment of bridges has been gradually adopted due to the limitation of elastic models to predict the failure mechanisms of bridges. Force-based methods are traditionally used in common practice by employing a simple analysis which takes into consideration inelastic response based on the seismic response modification factor provided by bridge codes. Modeling solutions provided by current software tools include a variety of nonlinear procedures, making them available to structural engineers, but a survey of seismic safety assessment of existing steel buildings conducted by [7] showed that only 42% of practitioners in Portugal are familiarized with nonlinear static and dynamic procedures, and practical applications of such procedures are only carried out by 20% of those who are familiarized, it is not expected a situation better in Colombia than the situation at the present time in Portugal in this respect.

Modeling solutions provided by current software tools target the use of nonlinear analysis, but new normative documents prefer nonlinear static analysis over nonlinear time-history analysis. In addition, existing seismic safety assessment methodologies provided by various codes follow conceptually different approaches related to Performance-Based Design (PBD) concepts and greatly rely on nonlinear analysis procedures. [8] using state-of-practice software tools studied structural analysis software tools commonly used by structural engineers to conduct nonlinear analysis of bridge structures. Biaxial modeling of bridge components using fiber models are found to be more accurate when adaptive pushover analysis is used due to the inclusion of higher mode effects and structure degradation. The P213 PREC8 bridge [9] was used to model the nonlinear response of the bridge using the software tools Sap2000 [10] and the structural analysis software tool SeismoStruct (<http://www.seissoft.com>). Good matching was found in both static and dynamic nonlinear results when the results provided by the two software tools are compared. [8] additionally highlighted that the constant load pattern commonly used in conventional pushover analysis led to inaccurate response predictions and concluded that adaptive pushover analysis using fiber-based finite element modeling is a valid alternative approach to predict the nonlinear response of bridges. Seismic design must also address serviceability of bridges after a major earthquake event and not only focus on collapse avoidance by using performance levels in terms of damage states and design criteria. Several contributions have been made to define appropriate damage limit states mainly proposed to assess the performance of frame structures. Strain limit and interstory drift are the main parameters used by several researchers to define damage limit states. The Japanese Design Specifications for Highway Bridges [4] recommends multi-level seismic design using two levels of ground motion (Level 1 and Level 2). Level 1 is defined as the most probable earthquake to occur during the service life of the bridge targeting seismic performance to avoid structural damage and Level 2 is set to limited damage ensuring a rapid recovery after earthquake using two types of earthquake motion (Type I and Type II). Type I is associated to a ground motion from large-scale subduction-type earthquake and Type II is



associated to near-field shallow earthquakes. Damage limit states in reinforced concrete columns are defined as SPL2 (repairable limit state) and SPL3 (ultimate limit state) related to residual flexural cracks or minor spalling of cover concrete and condition just before buckling of longitudinal reinforcement, respectively. A new equation was incorporated in the revised version of the code in 2012 and was developed to estimate plastic hinge length in reinforced concrete columns. The main parameters used in the above mentioned equation are the yield strength of the longitudinal reinforcement, the diameter of the longitudinal reinforcement, the spring stiffness provided by the transverse reinforcement and the spring stiffness provided by concrete cover. In addition, reinforced concrete bridge columns with hollow sections must have a solid section in the plastic hinge regions and haunches must also be used at the four corners inside the hollow section [11]. [5] and [6] also adopted a multi-level seismic design using two-level design criteria defined by 475-year and 2475-year return periods. The damage limit states provided by the [5] are concrete compressive strain (ϵ_c) limited to 0.004 and steel strain (ϵ_s) limited to strain at yield for 475-year return period. The 2475-year return period damage limit states are defined by concrete compressive strain limited to ultimate compressive strain (ϵ_{cu}) and steel strain limited to 0.05. On the other hand, the damage limit states provided by the [6] are concrete compressive strain limited to 0.006 and steel strain limited to 0.01 for 475-year return period. The 2475-year return period damage limit states are defined by concrete compressive strain limited to 80% ultimate compressive strain (ϵ_{cu}) and steel strain limited to 0.05.

[12] conducted a thorough investigation using 10 bridge codes including the above mentioned bridge codes to review current practice of performance-based seismic design of bridges. It is highlighted by the authors that the consensus in bridge engineering has not been achieved in terms of design criteria and therefore a comparative study was conducted in order to analyze the design criteria adopted in 10 bridge design specifications. A static nonlinear procedure is used for comparison of different design code criteria showing that the Canadian Highway Bridge Design Code [5] is the most stringent bridge code. It is also important to note that according to the authors the bridge specifications [2] and [3] adopted a single level design using a 1000-year return period after rejecting a previously proposed two-level design criteria based on 100-year and 2500-year return periods. The Colombian Bridge Construction Code [1] adopted from [2] the multiple level design as not mandatory. [12] also recommend the use of innovative seismic design approaches such as base isolators and Buckling Restrained Braces (BRB). Finally, [12] noted that PBD opens the door to the development of structural systems that can perform better than bridge structures designed following existing code prescriptions. Recent events in Colombia had shown the necessity of implementing new design verification procedures in accordance with the [1]. Although the [1] allows multiple level design using multiple return periods depending on owners, bridges in Colombia are mainly designed using a single level design defined by the 1000-year return period adopted from [2] and [3]. The number of segmental bridges constructed in Colombia have increased in recent years. The Yatí-Bodega bridge was constructed to connect the Magangué with Mompox becoming in 2020 the largest bridge in South America with a total length of 2.3 Km, the bridge located over the Magdalena's river was constructed using the segmental bridge construction method. Urban bridges such as Moravia bridge and La Union viaduct are also examples of segmental bridge construction, these bridges are located in Medellín and Bucaramanga, respectively. La Union viaduct helped to significantly decrease traffic congestion in Bucaramanga and Floridablanca Municipalities. One special feature related to La Union viaduct is that the Bucaramanga nest is one of the most seismically active regions in the world and therefore special attention must be given to infrastructure construction. The objective of this study is to assess the seismic performance of a recently constructed segmental bridge called La Unión viaduct based on a fiber-based finite element model of the bridge using non-linear analysis to study the ductility capacity of the bridge and to evaluate the seismic response modification factor employed in the design. The damage state limits provided by [5] for multi-level seismic design are used to determine the level of performance of the bridge. Potential earthquake hazards in the bridge site are also considered to study the seismic performance of the bridge.



2. Case study

2.1 Bridge characteristics

The segmental bridge selected in this study corresponds to the main bridge structure of the La Union viaduct located in Bucaramanga, Colombia and having a central length of 111 m. and lateral lengths of 52.45 m and 55.5 m as shown in Fig. 1. The superstructure of the central bridge is supported by two pairs of columns. The geometry selected for the columns corresponds to a rectangular hollow prismatic with an external cross section of 6 m x 5 m, and an internal cross section of 5 m x 4 m, provided with a constant wall thickness of 0.5 m. The pair of columns are separated to each other at a center-to-center distance of 11.2 m, with a height of 22 m. The foundation system corresponds to a rectangular concrete reinforced structure of 20 m x 11 m, supported on a set of 15 piles of 1.5 m in diameter and lengths of 20 m and 25 m. The cross section of the bridge corresponds to a tricellular concrete box girder of varying height (2.5 m to 6 m) and constant width of 22.5 m as shown in Fig. 2.

2.2 Finite element model of the bridge

The information provided by the bridge owner (Government of the Department of Santander) was used to assemble the finite element model of the bridge. The weight of the materials was also taken from the above mentioned information. The modeling approach for the bridge was selected based on the modeling recommendations provided by [8]. Fiber-based finite element modeling is then used to assemble the FE model of the bridge using the software tool [13] and the modeling procedure proposed by [14]. Elastic frame elements are used to model the tricellular concrete box girder of the bridge, all superstructure loads are considered in the finite element model using the load values provided by the bridge owner, the compressive strength of concrete for the segmental beams is 35 MPa, Young's modulus is numerically determined in accordance with the recommendation provided by [1]. Detailed information regarding the double column supports of the bridge was used to assemble the fiber-based nonlinear finite elements of the double column supports. The specified compressive strength of concrete defined by the columns is 28 MPa. The connection of the double-column supports to the deck is modelled using the elastic element with increased torsional stiffness, the top beam is assumed to be rigid in the plane of the deck and the two double-column supports are assumed to be fixed at the base. Additional information related to the nonlinear modeling considerations can be found in [14]. Fig. 3 shows the finite element model of the bridge.

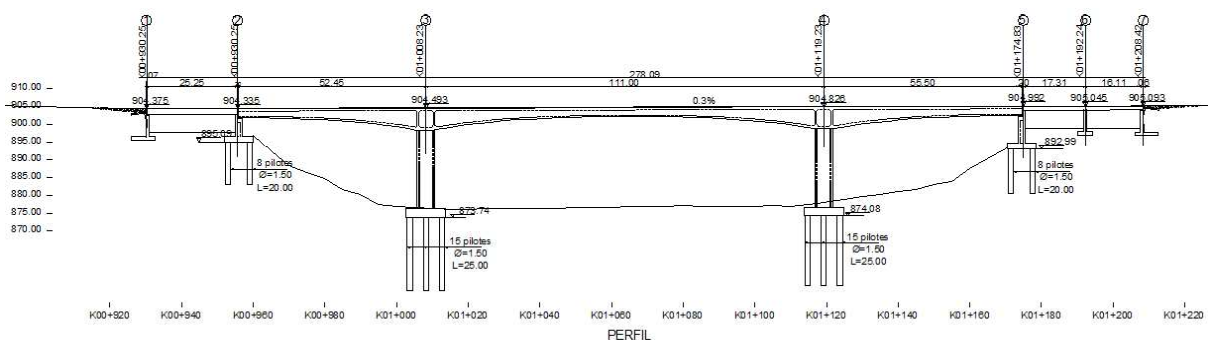


Fig. 1 – La Unión Viaduct (Side view). Source: Government of the Department of Santander.

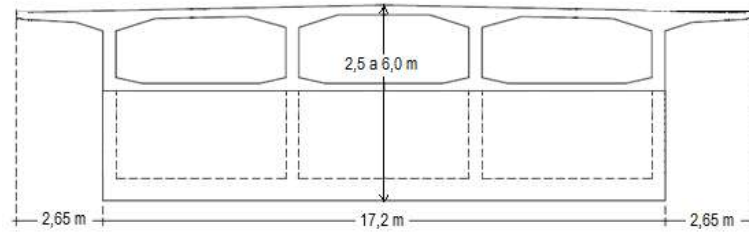


Fig. 2 – La Unión Viaduct (Cross-section). Source: Government of the Department of Santander.

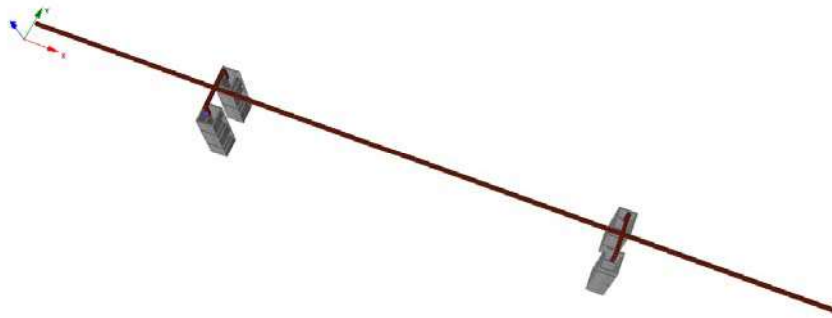


Fig. 3 – La Unión Viaduct (fiber-based nonlinear model). Source: The authors.

2.3 Seismic ground motions

[15] conducted a sensitivity analysis of a long stone bridge using near- and far- field earthquake records. Actual earthquake records were available to the bridge site and were used to study the response of the bridge under the action of a near-field earthquake. 4 real earthquake ground motions were used by the authors, 2 near-field ground motions and 2 far-field ground motions. One of the main conclusions derived from this study is that far-field earthquake effects are more severe than near-field earthquake effects of same peak ground acceleration, and damageability of earthquakes can be correlated to Arias intensity (IA). [15] pointed out that if the value of the input energy is larger than the dissipation capacity of the structure, progressive damage is expected to occur in the structure leading eventually to structural collapse. [16] conducted a seismic vulnerability study of a three-span continuous highway bridge using near-fault, far-field and long durations ground motions. Based on code regulations [17] near-fault earthquake is assumed in this study if the bridge is within 15 Km of a fault. [16] highlighted that near-fault motions are characterized by large ground displacements, peak velocities, and long period velocity pulse generating high input energy on structures. It is also mentioned that Arias significant duration (D_s) is an important parameter to differentiate near-fault and far-field earthquakes, D_s is then defined when the 90% of the seismic energy is carried by the time-history, commencing at the time at which the Arias intensity reaches a specified absolute level, 5% and 95% are commonly used to limit the time-history record. [16] defined long duration motions if the value of $D_{s5\%-95\%}$ is larger than 30 sec.

The seismic hazard at the bridge site is also considered based on the information provided by the bridge owner. In situ down-hole shear wave velocities are obtained before construction of the bridge. Shear wave velocities calculated down to a depth of 30 m (VS_{30}) varied between 371 m/s and 481 m/s. According to the seismological hazard defined by the bridge site, the earthquake environment of far-field earthquake effects and near-field earthquake effects are also identified in La Unión viaduct site.



Near-field earthquakes are therefore associated to the Bucaramanga-Santa Marta fault and far-field earthquakes are associated to the Piedemonte llanero fault. The selection of representative earthquake records must satisfy the following magnitude and fault distance range conditions: near-fault ground motions $M_w=[5.6-6]$ and $R=[13-25]$ Km and far-field ground motions $M_w=[6.8-7.5]$ and $R=[60-80]$ Km. As previously mentioned, [1] adopted a single level design using a 1000-year return period, the software tool [13] is used to select ground motions records according to the above mentioned parameters and perform the respective adjustment to the elastic target spectrum defined by the [1]. 3 near-fault and 3 far-field ground motions are then acquired from Pacific Earthquake Engineering Research (PEER) Centre earthquake database [19] based on the matching and scaling results provided by the software tool [18]. $DS_{5\%-95\%}$ values are computed using the software tool Deepsoil [20]. Table 1 shows the characteristics of the selected near-fault and far-field ground motions. Fig. 4 and 5 show the selected ground motions and elastic target spectrum for the near-fault and far-field ground motions, respectively. The Iwate RSN 5492 is the only record that can be defined as long duration ground motion according to [16].

Table 1 – Characteristics of the selected ground motions. Source: The authors.

RSN	Earthquake	Station	Year	PGA(g)	R (Km)	$DS_{5\%-95\%}$	V_{S30} (m/s)	Scal. Fact.
4130	Parkfield	Cany 1E	2004	0.30	18.76	6.315	381.27	1.00
4132	Parkfield	Cany 2E	2004	0.26	19.64	5.750	467.76	1.27
4075	Parkfield	W.Ranch	2004	0.30	13.18	2.765	446.50	1.51
5671	Iwate	MYG012	2008	0.10	79.70	24.21	407.86	3.27
5239	Chuetsu-oki	NGNH29	2007	0.10	71.88	18.62	464.92	3.48
5492	Iwate	AKTH16	2008	0.11	73.10	41.19	375.00	3.16

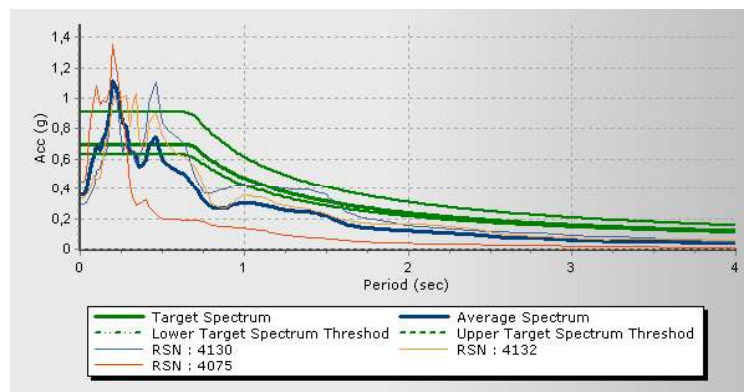


Fig. 4 – Target spectrum CCP-14 for the near-fault ground motions. Source: The authors.

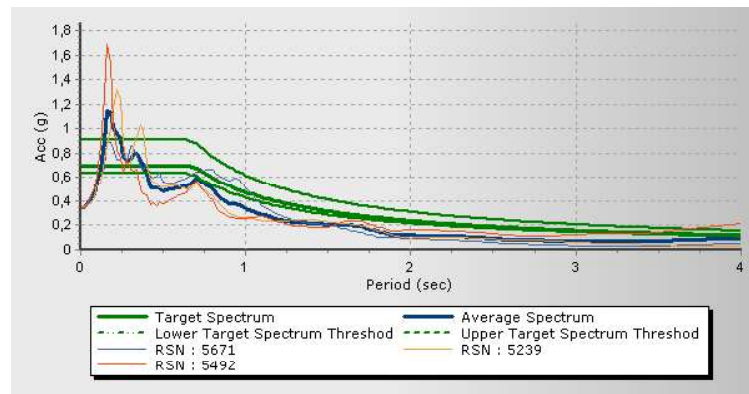


Fig. 5 – Target spectrum CCP-14 for the far-field ground motions. Source: The authors.

3. Nonlinear analysis

3.1 Static analysis

Based on the recommendations provided by [8] an adaptive pushover analysis is selected in order to conduct the seismic performance assessment of La Union viaduct using the prescriptions provided by the [5]. The inelastic base shear (V_{sd}) is obtained, at each load step, through a series of lateral loads applied to the bridge, when the bridge reaches a determined damage limit state the value of the corresponding inelastic base shear is computed. Fig. 6 and 7 show the inelastic base shear (V_{sd}) vs displacement of a single column in the longitudinal and transverse directions, respectively. Table 2 shows the code comparison in terms of the design criteria provided by [5] and [6] based on the concrete compressive strain (ϵ_c), the ultimate concrete compressive strain (ϵ_{cu}) and steel strain (ϵ_s) for 475-year and 2475-year return periods.

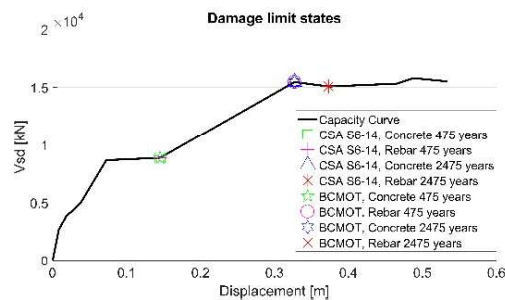


Fig. 6 – Capacity curve (longitudinal direction). Source: The authors.

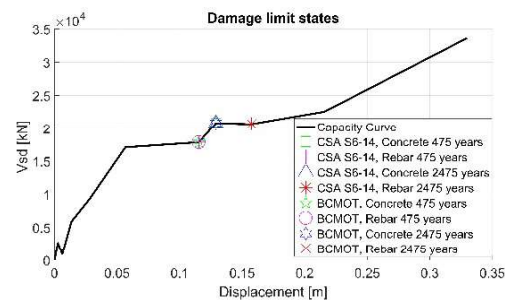


Fig. 7 – Capacity curve (transverse direction). Source: The authors.



Table 2 – Code comparisons in terms of damage limit states longitudinal direction. Source: The authors.

Code	Criteria	V_{sd} (kN)	Lat. disp. (m)	Drift (%)
CSA S6-14, Rebar 475 years	$\epsilon_s \leq \text{yielding}$	8859.941	0.145	0.66
CSA S6-14, Concrete 475 years	$\epsilon_c \leq 0.004$	8859.941	0.145	0.66
CSA S6-14, Rebar 2475 years	$\epsilon_s \leq 0.05$	15076.96	0.373	1.70
CSA S6-14, Concrete 2475 years	$\epsilon_c \leq \epsilon_{cu}$	15456.42	0.327	1.49
BCMOT, Rebar 475 years	$\epsilon_s < 0.01$	15456.42	0.327	1.49
BCMOT, Concrete 475 years	$\epsilon_c \leq 0.006$	8859.941	0.145	0.66
BCMOT, Rebar 2475 years	$\epsilon_s \leq 0.05$	15076.96	0.373	1.70
BCMOT, Concrete 2475 years	$\epsilon_c \leq 80\% \epsilon_{cu}$	15456.42	0.327	1.49

Table 3 – Code comparisons in terms of damage limit states transverse direction. Source: The authors.

Code	Criteria	V_{sd} (kN)	Lat. disp. (m)	Drift (%)
CSA S6-14, Rebar 475 years	$\epsilon_s \leq \text{yielding}$	17832.46	0.115	0.52
CSA S6-14, Concrete 475 years	$\epsilon_c \leq 0.004$	20778.19	0.129	0.59
CSA S6-14, Rebar 2475 years	$\epsilon_s \leq 0.05$	20664.62	0.158	0.72
CSA S6-14, Concrete 2475 years	$\epsilon_c \leq \epsilon_{cu}$	20778.19	0.129	0.59
BCMOT, Rebar 475 years	$\epsilon_s < 0.01$	17832.46	0.115	0.52
BCMOT, Concrete 475 years	$\epsilon_c \leq 0.006$	17832.46	0.115	0.52
BCMOT, Rebar 2475 years	$\epsilon_s \leq 0.05$	20664.62	0.158	0.72
BCMOT, Concrete 2475 years	$\epsilon_c \leq 80\% \epsilon_{cu}$	20778.19	0.129	0.59

In the longitudinal direction, it is possible to observe that the bridge reaches the 475-year return period limit state due to concrete strain for both codes [5] and [6]. In the transverse direction, the bridge reaches the 475-year return period limit state due to rebar strain for both codes [5] and [6]. The analysis of the results for the 2475-year return period indicates that the bridge exhibits higher ductility in the longitudinal direction than in the transverse direction.

3.2 Time history analysis

As previously mentioned, [1] recommends a single level design defined by the 1000-year return period adopted from [2] and [3]. To study the seismic performance of the bridge using the elastic target spectrum defined by [1], the 6 scaling ground motions previously obtained are applied to the fiber-based finite element model of the bridge for the seismic level design recommended by [1]. The maximum value of the inelastic base shear (V_{sd}) obtained from each time history response of a single column is used to determine if the column has reached the design criteria values provided in Tables 2 and 3. As previously mentioned, the bridge must have adequate capacity to carry traffic in order to provide serviceability after the occurrence of an earthquake, the adaptive pushover analysis showed that the bridge reached the serviceability limit in the longitudinal direction at a lower value of V_{sd} . Although the serviceability limit is higher in the transverse direction, ductility is lower in that direction. Tables 4 and 5 show the maximum values of the inelastic base shear (V_{sd}) for a single column obtained from the scaling ground motions.



Table 4 – Nonlinear time history response (longitudinal direction). Source: The authors.

RSN	Earthquake	Station	Ds _{5%-95%}	Scal. Fact.	V _{sd} (max.) (kN)
4130	Parkfield	Cany 1E	6.315	1.00	7800.858
4132	Parkfield	Cany 2E	5.750	1.27	7267.304
4075	Parkfield	W.Ranch	2.765	1.51	5013.781
5671	Iwate	MYG012	24.21	3.27	9524.102
5239	Chuetsu-oki	NGNH29	18.62	3.48	7467.209
5492	Iwate	AKTH16	41.19	3.16	15525.37

Table 5 – Nonlinear time history response (transverse direction). Source: The authors.

RSN	Earthquake	Station	Ds _{5%-95%}	Scal. Fact.	V _{sd} (max.) (kN)
4130	Parkfield	Cany 1E	6.315	1.00	10378.62
4132	Parkfield	Cany 2E	5.750	1.27	13706.77
4075	Parkfield	W.Ranch	2.765	1.51	8460.120
5671	Iwate	MYG012	24.21	3.27	15450.93
5239	Chuetsu-oki	NGNH29	18.62	3.48	13928.35
5492	Iwate	AKTH16	41.19	3.16	12669.56

The adaptive pushover results show that in the longitudinal direction the serviceability limit state corresponds to a value of $V_{sd}=8859.941$ kN and the ultimate limit state corresponds to a value of $V_{sd}=15076.96$ kN. The effects of near-fault ground motions are located below the serviceability limit, but the effects of far-field ground motions are located above the serviceability limit and in the case of the ground motion with the largest Ds 5%-95%, the corresponding value of V_{sd} is similar to the limit state value. In the transverse direction the serviceability limit state corresponds to a value of $V_{sd}=17832.46$ kN and the ultimate limit state corresponds to a value of $V_{sd}=20664.62$ kN. The results obtained from the nonlinear time history analysis show that the serviceability limit state defined by either [5] or [6] is not reached for the design level defined by the 1000-year return period in the transverse direction. These findings are similar to the ones found by [15] related to the fact that far-field earthquakes are far more destructive than their near-fault counterparts. Finally, it is important to note that the static nonlinear analysis provides useful information to more adequately interpret the results from nonlinear time history analysis due to the determination of the ductility level of the bridge, the case study shows significant differences in bridge performance depending on the direction of action of the scaling ground motions.

4. Conclusions

Seismic assessment of a newly constructed segmental bridge is presented. Nonlinear analysis is conducted using a fiber hinge finite element model to study the inelastic response of the bridge columns. The multiple level design criteria proposed by the codes [5] and [6] is used to verify the seismic performance of La Union viaduct. The adaptive pushover analysis results show ductility reserve after reaching the serviceability limit in the longitudinal direction. However, the ductility level is very limited in the transverse direction reaching the ultimate limit state soon after the serviceability limit is achieved. This result is in accordance with the value of the seismic modification factor ($R=1.0$) used in the design. The nonlinear time history time results show adequate seismic performance of the bridge columns.



It was also possible to verify the seismic performance of the bridge at the serviceability level using the design level defined by the 1000-year return period. No damage is induced in the columns due to the effect of the scaling ground motions acting on the bridge. Nevertheless, the design level defined by the 2475-year return period recommended by the [5] and [6] was not verified due to fact that the [1] does not provide seismological hazard information for the bridge site. Nonlinear analysis provides valuable information to validate the seismic response modification factor used in the design and early detect deviations from code regulations in order to adopt prompt actions to improve the seismic performance of the bridge or apply innovative solutions such as the ones mentioned in this study. Nonlinear analysis procedures have the potential to produce bridge structures to be rapidly repaired during the occurrence of an earthquake, even in cases where the return period level is achieved.

5. Acknowledgements

The authors gratefully acknowledge the support of the government of the Department of Santander and the research group INME, School of Civil Engineering, Industrial University of Santander and the University of Antioquia.

6. References

- [1] AIS (Asociación Colombiana de Ingeniería Sísmica). (2014). *Norma Colombiana de Diseño de Puentes CCP-14*.
- [2] AASHTO. (2014). *AASHTO LRFD bridge design specifications*. Washington, DC: American Association of State Highway Transportation Officials.
- [3] AASHTO. (2013). *AASHTO guide specifications for LRFD seismic bridge design*. Washington, DC: American Association of State Highway Transportation Officials.
- [4] Japan Road Association (JRA). *Specifications for Highway Bridges, Part I_V*, 2012.
- [5] CSA S6-14. *Canadian Highway Bridge Design Code (CHBDC)*. (2014). Canadian Standards Association.
- [6] BCMOT. (2016). *British Columbia Supplement to CHBDC S6-14*. Victoria: British Columbia Ministry of Transportation and Infrastructure.
- [7] Araújo, M., Castro, J.M. (2018). A critical review of European and American provisions for the seismic assessment of existing steel moment-resisting frame buildings. *Journal of Earthquake Engineering*, 22(8), pp. 1336-1364.
- [8] Monteiro, R., Araújo, M., Delgado, R., Marques, M. (2018). Modeling considerations in seismic assessment of RC bridges using state-of-practice structural analysis software tools. *Front. Struct. Civ. Eng.*, 12(1), pp. 109-124.
- [9] Kohrangi M, Bento R, Lopes M. (2015). Seismic performance of irregular bridges - comparison of different nonlinear static procedures. *Structure and Infrastructure Engineering*. 11(12), pp. 1642–1650.
- [10] CSI. (2010). *CSI Analysis Reference Manual for SAP2000. ETABS and SAFE*, Computer and Structures, Inc, California.
- [11] Kuwabara, T., Tamakoshi, T., Murakoshi, J., Kimura, Y., Nanazawa, T., & Hoshikuma, J-I. (2013). Outline of Japanese design specifications for highway bridges in 2012. Paper presented at *the 44th Meeting, Joint Panel on Wind and Seismic Effects (UJNR)*, UJNR Gaithersburg.
- [12] Zhang, Q., Shahria Alam, M. (2019). Performance-based seismic design of bridges: a global perspective and critical review of past, present and future directions. *Structure and Infrastructure Engineering*, 15(4), pp. 539-554.
- [13] SeismoSoft. (2020). *SeismoStruct* (version 2020) [Computer software]. Italy: SeismoSoft, Pavia.
- [14] Serdar, N., Folić, R. (2018). Vulnerability and optimal probabilistic seismic demand model for curved and skewed RC bridges. *Engineering Structures*, 176, pp. 411-425.



- [15] Simos, N., Manos, G., Kozikopoulos, E. (2018). Near- and far-field earthquake damage study of the Konitsa stone arch bridge. *Engineering Structures*, 177, pp. 256-267.
- [16] Rashedul Kabir, Md., Muntasir Billah, A.H.M., Shahria Alam, M. (2019). Seismic fragility assessment of a multi-span RC bridge in Bangladesh considering near-fault, far-field and long duration ground motions. *Structures*, 19, pp. 333-348.
- [17] Caltrans. *Seismic design criteria*. (2004). Sacramento, CA: California department of transportation.
- [18] SeismoSoft. (2020). *SeismoSelect* (version 2020) [Computer software]. Italy: SeismoSoft, Pavia.
- [19] PEER (Pacific Earthquake Engineering Research). (2011). New ground motion selection procedures and selected motions for the PEER transportation research program. Berkeley, CA: *University of California*; 2011.
- [20] Hashash, Y.M.A., Musgrove, M.I., Harmon, J.A., Ilhan, O., Groholski, D.R., Phillips, C.A., and Park, D. (2017). "DEEPSOIL 7.0, User Manual".